

## REMARKS

Office action mailed 5/13/2004 noted that no FIG. 15 was included. Applicant has corrected this error by changing FIG. 14A to FIG. 14 and changing FIG. 14B to FIG. 15.

Respectfully submitted

A handwritten signature in black ink, appearing to read "John R. Ross", written in a cursive style.

John R. Ross

Regis. No.:30,530

Trex Enterprises Corporation

10455 Pacific Center Court

San Diego, CA 92121-4339

Phone: 858-646-5488

FAX: 858-646-5581

*Marked - up pages show corrections*

interrogator beam. One can achieve this goal by separating the retro-reflectors in the transverse (perpendicular to the optical axis) or in the longitudinal, or beam propagation, direction.

The lateral coherence diameter, or Fried parameter, depends on the vertical profile of the refractive index structure characteristic  $C_n^2(h)$  and elevation angle,  $\varepsilon$ , and it is given by

$$r_0 = \left[ 0.423(2\pi/\lambda)^2 (\sin \varepsilon)^{-1} \int_{h_0}^H C_n^2(z) dz \right]^{-3/5}$$

where  $H$  is the altitude of the interrogator, and  $h_0$  is the altitude of the array of MRRs. For HV<sub>57</sub> turbulence model  $r_0 = 5\text{cm}$  for  $\lambda = 0.5\mu\text{m}$  and propagation at the zenith. For  $\lambda = 1.55\mu\text{m}$  and  $\varepsilon = 90^\circ$ , the lateral coherence diameter is  $r_0 = 20\text{cm}$ , whereas for  $\varepsilon = 30^\circ$ ,  $r_0 = 13\text{cm}$ . For daytime turbulent model the Fried parameter is  $r_0 = 8.6\text{cm}$ . Thus, if the modulated retro-reflectors are separated at the distance  $\Delta l > 20\text{cm}$ , then each retro-reflector will be located in a different coherent volume and coherent interference between the retro-reflected beams will be eliminated.

In addition, the longitudinal coherence length,  $l_c = \frac{\lambda^2}{2\Delta\lambda}$ , is determined by the wavelength,  $\lambda$ , and the laser line width,  $\Delta\lambda$ . For  $\lambda = 1.55\mu\text{m}$  and line width of  $\Delta\lambda = 1.0\text{nm}$ , the longitudinal coherence length is  $l_c = 1.2\text{mm}$ . Therefore, if the spacing between the retro-reflectors in the longitudinal direction exceeds 1.2 mm, the longitudinal coherence length,  $\Delta l_l > l_c$ , then each retro-reflector will be located in a different coherent volume. This will prevent coherent interference between the retro-reflected beams.

## Technical Details for the Dynamic Modulated Retro-Reflector Design

### Retro-Reflector Lens Design

The preliminary retroreflector design is based on a refractive optical system with a curved mirror at the focal plane, as shown in FIG. 14~~A~~<sup>15</sup> and B. The modulator is placed

near the focal plane, so all the incoming light is concentrated into a small area. The instantaneous field of view of the optical system is determined by the modulator diameter and the lens focal length.

Assuming a 6 mm diameter modulator, and an 86 mm focal length, the instantaneous field of view is  $4^\circ$ . A reasonable focal ratio of F/2.4 leads to an input aperture of 36 mm. This is much larger than any cat's-eye design with a similar focal length. The field of regard for this simple doublet with a primary mirror is 120 degrees. FIGS. 14~~A~~<sup>15</sup> and ~~B~~<sup>15</sup> show two ray bundles, one at 60 degrees off-axis, and one on-axis, are shown. The modulator near the mirror is not shown in the FIG. 14~~B~~<sup>15</sup> view.

We have designed a preliminary system to show the essential details. The simple doublet shown in FIGS. 14~~A~~<sup>15</sup> and ~~B~~<sup>15</sup> provides a diffraction-limited retro-reflection over a field larger than about 6 degrees (or 12 degrees with a 25 mm aperture). This field can be increased to about 120 degrees by adding additional optical surfaces and selecting appropriate optical glasses. For example, some fisheye lenses for 35 mm cameras have been designed with fields of view exceeding 180 degrees, all while maintaining color correction over the entire visible spectrum. The lens required here differs in that only monochromatic color correction is required, freeing up those surfaces and materials to aid in improving the wave front quality. In addition, instead of requiring a flat focal plane, we need a curved surface that is normal to the incoming beam. We can use an aspheric surface for this optic, so the lens focal length does not have to be fixed across the entire field of view. Finally, we do not require a fixed field stop; we will optimize the design to use as large an aperture as possible. The modulator position near the mirror is shown in FIG. 14~~A~~<sup>15</sup> by a small black bar. Note that vignetting is minimized by keeping the bar parallel to the mirror surface. Not shown is the glass layer in front of the reflective surface.

The optimization merit function, which the ray tracing program automatically minimizes to find the best optical solution, will be weighted to emphasize the edge of the field of view. This is where the communication range is the longest (20 km) and the effective

aperture is the smallest. For light coming in on-axis, the maximum range is only 10 km, so the retro-reflected signal is roughly 16 times stronger. If the optical design shows good performance on-axis, this will result in good communication under more adverse conditions. This type of tradeoff will be studied during lens optimization.

While an all-spherical design is desired, it might be necessary to place a simple asphere on some lens surfaces. Molded plastic or glass lenses are now routinely used in the commercial world, so this aspect should not restrict the design. The goal is to produce a design with the largest possible aperture, but some tradeoffs with manufacturability must always be considered.

The design should also be rugged and work over a wide temperature range. The spacing between the lenses and the mirror is critical. For best performance in this retro-reflecting system, the focus error should be on the order of the wavelength times the square of the focal ratio, or about 10 microns. This can easily be held with the appropriate spacer materials; Invar or silica, for example, are adequate. Depending on the actual glasses used in the final design, their effect on the focal length might also have to be considered in the overall compensation equation. Passive thermallization is always desired, but since some feedback from the airborne interrogator is possible, active thermallization might also be considered to further enhance performance.

Finally, if it is necessary to protect the reflecting surface from dust and contamination that might reduce retro-reflective efficiency, two alternatives are presented. The baseline approach is to make the mirror a second surface Mangin type. The mirror is not too large, so that BK7 can be used as a substrate, and a reflective coating applied to the back side. The reflection then goes through the glass, and any dust or contaminants on the first surface would be out of focus. Since that refractive surface is close to focus, its shape is not too critical, and a simple concentric surface should be acceptable. The back side reflector could be a gold coating, protected with a lacquer layer.

The alternative design, if the mirror is made of some low-expansion glass that does not transmit well, is to use a hard dielectric first surface mirror and use an anti-static type brush around the modulator aperture to keep the surface swept clean. As the modulator moves around the surface, the soft brush would sweep away dust, assuring that the reflection is always perfect.

### Modulator Design

Applicants' preferred modulator for the retro-reflectors shown in FIGS. 2 and 14~~A~~ are 6 mm diameter modulator according to the description in the '299 patent referred to in the Background Section and incorporated herein by reference. These modulators are available from the Naval Research Laboratories. Other modulators may be used. The key requirements include a small package, low power consumption, and 45 MHz modulation capability.

Applicants' preferred embodiments includes optical tracking. Assuming the modulator diameter is 6 mm, the tracking requirements are easy to meet. An error of 1 mm would cause a negligible decrease in signal, so a precision tracking system is not required. The tracking camera presented in the next section can handle an angular tracking motion of 24 degrees per second. On the mirror surface, this corresponds to traversing the mirror surface in 5 seconds. For the mirror shown here, the maximum velocity would be only 28 mm/sec. Normally, the motion would be much slower.

Two mechanical designs have been considered: one uses cables to directly pull the modulator on hinged rails placed near the mirror; the alternate design uses magnetic coupling through the mirror to pull the modulator anywhere on the surface, without rails.

The baseline design uses rails to guide the modulator, as shown in FIG. 16. The modulator is shown as a 50 mm wide board, but the actual active aperture would only be large enough for the optical beam to pass through. Each end of the board is attached to cables connected to miniature motors set up like the mechanisms on common ink jet

printers or older X-Y chart recorders. To allow access to any part of the mirror's surface, each end of the rail must be hinged. (Both rails are actually split into two parts so that the optical beam can pass between them.) The orthogonal rail will then be free to drive the modulator along the spherical surface. Since accuracy is not a major concern, the guides can be loose enough to prevent binding in any conceivable circumstance.

One advantage of this design is that the optics are never touched, preserving the optical alignment and the mirror surface for good retro-reflections. The main disadvantage is that the rails are somewhat difficult to design, or align. A rail-less system is shown in FIG. 17, where magnets act through the glass to move the modulator.

Taking advantage of the curved back surface, a few strong magnets can be positioned anywhere on the surface with a few opposing cables. A pair of rare earth magnets only 19 mm diameter can easily work through a substrate 50 mm thick, as long as the friction is not too large. The modulator board would be supported over the mirror by small rolling sapphire spheres or Teflon pads. Even if the mirror were a first surface design, durable hard-coated dielectric mirrors can easily survive this type of friction.

The advantage of this type of design is that it is more reliable. The primary disadvantage is the potential problem of scratches appearing on the reflective surface. Since all the mechanical parts are on the back side, however, the optical chamber can be assembled and sealed in a clean room, preserving the optical cleanliness. The tradeoffs between these motion control choices will be studied in more detail once the optical design has been finalized, in case that design discourages the Mangin mirror approach.

The modulator board is shown with no direct connections to signal or power supplies. In either option presented so far, a thin flexible cable could be used to connect the modulator board, or even a fiber optic cable. A flexible service loop could be located near the chamber walls, and springs could be used to keep the slack from getting in the way of the optical beam. In Applicants' preferred approach, however, Applicants are presenting a wireless link to provide both power and signal. This approach seems

reasonable, especially since the requirements over such a short range seem simple to implement. This wireless option reduces risk and enhances reliability by reducing the number of moving or flexible components. The wireless transmitter is shown at 50 in FIG. 18 as the box in the upper left corner.

Getting a 45 MHz signal to the board is relatively simple, using a diffused laser source as a signal transmitter. A quick calculation shows that if a 3 mW-laser at 850 nm floods the optical chamber, a  $10 \text{ mm}^2$  silicon detector will pick up about 1 microwatt of laser power, or about 1000 times its noise level. This is more than enough margin to assure error-free signal transmission.

Inductive power coupling is used in a wide variety of consumer goods to provide power to electric razors and toothbrushes, as well as computer accessories. Normally, the wireless component runs on batteries that are kept charged while the unit is docked to the charging station. Since the modulator here may be turned on for a long period, we are assuming that our power requirements are continuous. The modulator board would only have a small capacitor storage cell that would operate the modulator for perhaps one or two seconds. This would reduce weight on the board, and by eliminating batteries, would enhance reliability. Power transfer over the entire range of the modulator motion is inefficient compared to close-coupled transfers, but the power requirements are expected to be so small that this inefficiency is not important.

An alternative to inductive coupling is using a solar cell on the board that picks up light from a bright LED. This is relatively inefficient because the light must be spread all across the field of regard, and only a small fraction can be captured. This light might also cause problems for the communication signal, although with appropriate filters, this could be a small effect. A few bright LEDs could provide 10 microwatts from a  $40 \text{ mm}^2$  solar cell.

ANNOTATED

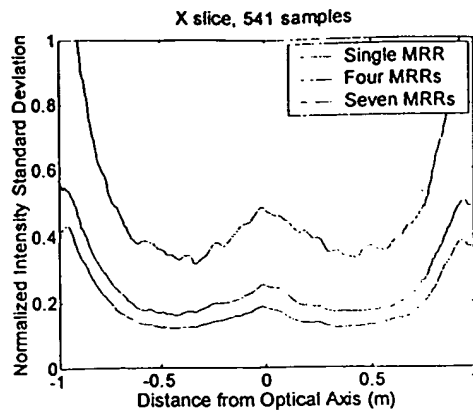


FIG. 12A

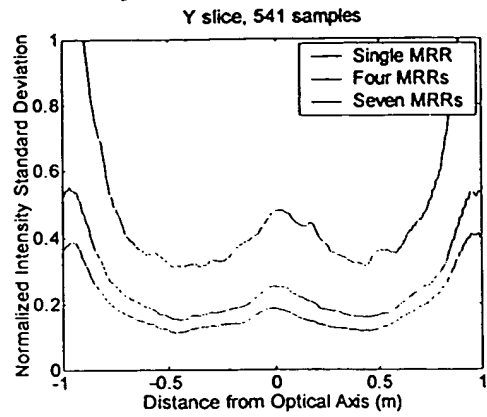


FIG. 12B

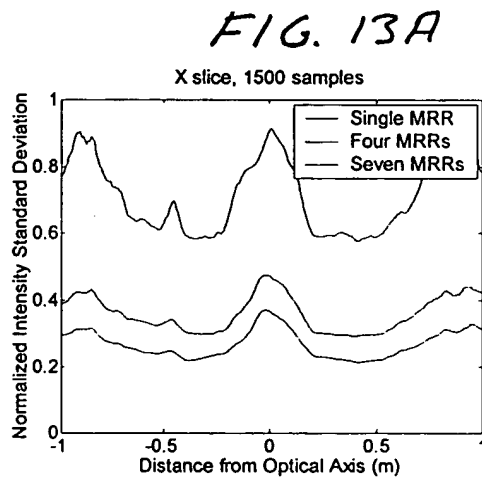


FIG. 13A

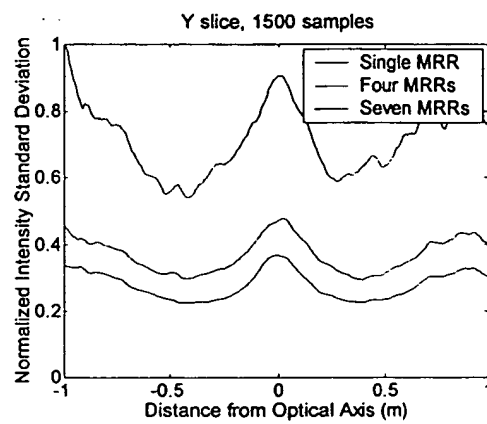


FIG. 13B

